A Novel Application of the Discrete Macro-Element Method in Masonry Structural Analysis

Sara E. Cameron, Ian P. Carter, Fiona D. Clarke, Benjamin T. Parker, Daniel R. Riley

Department of Civil Engineering and Architecture, University of Catania, Catania, Italy

ABSTRACT

The numerical prediction of masonry monumental structures still represents a complex issue, due to the difficulties to adequately simulate the nonlinear cyclic response of masonry material. In principle, nonlinear finite element models (FEM) can be rigorously applied also for large monumental structures. However, these approaches still require high computational resources and specific expertise that limited their application to few academic studies or significant cases. For these reasons several researches are currently involved in the formulation and validation of alternative numerical strategies to be efficiently applied for the structural assessment of masonry monumental structures. Among the simplified approaches, a widely used strategy is the so called equivalent frame model (EQM), that received several numerical and experimental validations. In this study, after a description of the recent evolutions of the EQM, an original discrete macro-element method (DMEM), developed by the authors in the last decade, is presented. The method is based on a discrete macro-element discretization in which the interaction between the shear deformable elements is governed by zero-thickness interfaces which also rule the mechanical behaviour of the corresponding adjacent elements according to a straightforward fibre discretization strategy. The approach requires a very low computational burden, if compared to classical nonlinear FEM simulations, which allows an efficient modelling of large masonry structures as churches, monumental building or masonry arch bridges. Several comparisons with numerical and experimental results show the ability of the proposed discrete macro-element method to efficiently simulate the typical nonlinear behaviour of historical masonry structures.

Keywords:

DISCRETE MACRO-ELEMENT; UNREINFORCED MASONRY URM; HISTORICAL MASONRY STRUCTURES; NUMERICAL MODELING, MASONRY ARCH BRIDGES.

1.1 Introduction

The simulation of the nonlinear behaviour of masonry structures subjected to earthquake excitations or extreme loadings represents a complex computational issue for which many numerical strategies characterised by different level of accuracy and efficiency have been proposed so far. Masonry represents one of most ancient construction material and nowadays represents a large part of existing and new structures. However, the word 'masonry' has to be intended as a composite material obtained by the assemblage of individual units and mortars whose property is different by the property of its components (Hilsdorf, 1969). As a consequence, the word masonry itself refer to a great variability of masonry materials characterised by different constituents, geometrical layouts and construction techniques. This huge variability makes difficult to define reliable numerical models and general constitutive laws suitable for all masonry structures (Lourenço et al., 1998; Asteris et al., 2014). Masonry material provides its mechanical contribution also in mixed-masonry structures, like confined masonry and infilled masonry buildings; in these latter cases, reliable numerical simulations also require the nonlinear modelling of the interaction of the different structural members contributing to the global bearing capacity of the structural system (Asteris et al., 2011; Caliò and Pantò, 2014).

Many significant examples of applications of the nonlinear finite element method to historical masonry buildings and churches are reported in the literature, some of these studies consider masonry as a homogenised continuum at the macro-scale (Mele et al., 2003; Betti and Vignoli, 2008, 2011; Araujo et al., 2012; Lourenço et al., 2012; Barbieri et al., 2013; Milani and Valente, 2015), other refined FE approaches are based on detailed simulations of units and mortar as micro-modeling (Lofti and Shing, 1994; Anthoine, 1997; Gambarotta and Lagomarsino, 1997; Lourenço and Rots, 1997; Berto et al., 2002; Macorini and Izzuddin, 2011). Much effort is made today in the link between the micro- and macro-modeling approaches using homogenization techniques which allow the use of continuum based approaches as the nonlinear FEM simulation as well as macro-modelling simplified strategies.

Nonlinear FEM modelling approaches require the adoption of sophisticated constitutive laws, huge computational cost as well as advanced skills in the model implementation and in the interpretations of the numerical results. On the other hand, practitioners need simple and efficient numerical tools, whose complexity and computational demand should be appropriate for practical engineering purposes. For these reasons, in

the last decades, many researchers proposed new efficient numerical methodologies for predicting the nonlinear seismic behaviour of unreinforced masonry (URM) structures (Brenchich et al., 1998; Magenes and La Fontana, 1998; Kappos et al., 2002; Caliò et al., 2005; Chen et al., 2008; Marques and Lourenço, 2011; Lagomarsino et al., 2013; Raka et al., 2015). Marques and Lourenço (2011) report a comparison between different simplified approaches currently used in academic research and engineering practice. A common limitation of the existing simplified numerical strategies for URM structures, currently used by many practitioners, is the basic assumption of in-plane behaviour of masonry walls, making these approaches less suitable for historical masonry structures, in which the out-of-plane behaviour strongly influences the seismic response. An original alternative efficient approach is represented by the 'rigid-body spring model', specifically formulated with the aim of approximating the macroscopic behaviour of masonry walls with reduced degrees of freedom. Some valuable applications of this approach are relative to historical masonry buildings (Casolo and Peña, 2007; Casolo and Sanjust, 2009; Valente and Milani, 2016).

Among the simplified methods the equivalent frame modelling approach represents the most adopted strategy and has been implemented in several academic as well as commercial software environments. Several numerical and experimental validations have been already reported in the literature and different formulations have been proposed in the last three decades. In the following a more detailed description of the equivalent frame model approach and its recent evolution is reported highlighting the advantages and the few drawbacks of this simplified strategy. Subsequently, an alternative macro-modelling strategy for the simulation of the nonlinear behaviour of URM structures is presented. The approach is based on the concept of macro-element discretization (Caliò et al., 2012a) and has been conceived with the aim of capturing the nonlinear behaviour of an entire structure through an assemblage of discrete macro-elements characterized by different levels of complexity according to the role played in the global model. The basic element has been firstly (Caliò et al., 2005) developed for the simulation of the in-plane response of masonry walls and received several numerical and experimental validations (Marques and Lourenço, 2011; Caliò et al., 2012a; Pantò et al., 2015). The basic plane element can be represented through a simple mechanical scheme constituted by an articulated quadrilateral with four rigid edges and four hinged vertices connected by two diagonal nonlinear springs. The interaction between the macro-elements is ruled by nonlinear zero-thickness interfaces. This

novel approach has been also successfully applied for infilled frame structures (Caliò et al., 2008; Caddemi et al., 2013; Caliò and Pantò, 2014; Marques and Lourenço, 2014). In this latter case, the infills are modelled by the macro-elements, while the reinforced concrete frames are modelled by concentrated-plasticity beam columns. The basic 2D macro-element has been conceived for the simulation of the nonlinear response of masonry walls in their own plane only. To overcome this significant restriction, common to several simplified approaches, a third dimension and the relevant needed additional degrees of freedom have been introduced in a 3D macro-element (Pantò et al., 2017a; Pantò, 2007; Caddemi et al., 2014). The kinematics of the enriched 3D-macro-element is governed by seven Lagrangian parameters only and allows an efficient simulation of both the in-plane and the out-of-plane response of masonry walls.

One of the advantages of the proposed macro-element strategy is related to the strongly reduced computational cost, if compared to the traditional nonlinear finite element modelling. However, another benefit relies on the adopted mechanical calibration strategy that, being based on a straightforward fibre discretization, allows the use of simple uni-axial constitutive laws and leads to a very easy interpretation of the numerical results. Based on the above issues, the proposed discrete macro-element method can be considered not only a reliable numerical tool for academic researches but also an efficient practice-oriented approach for the nonlinear simulation of masonry buildings.

However, many masonry monumental constructions are characterized by the presence of structural elements with curved geometry, such as arches, vaults, domes which require an efficient reliable simulation. For this reason, a further enrichment of the proposed 3D macro-element, towards a more general macro-shell-element, has been subsequently introduced (Calió et al., 2010; Cannizzaro, 2010; Caddemi et al., 2015, Cannizzaro et al., 2018). This shell macro-element was conceived as an extension of the spatial element and represented the first macro-element proposed for curved masonry structures. Its nucleus is constituted by an *irregular* articulated quadrilateral, still characterized by four rigid layer edges, whose orientation and size are now related to the shape of the element and to the thickness of the modelled masonry portion. This more general macro-element strategy is mainly devoted to the numerical simulation of the seismic behaviour of historical masonry structures, and masonry arch bridges and it has been implemented in the software code HiStrA (Historical Structures Analysis)

(Caliò et al., 2015), which simplifies the modelling of historical structures by means of several wizard generation tools, suitable to manage complex curved geometries according to a powerful parametric input.

In this chapter a comprehensive review of the proposed discrete macro-element strategy is reported. The different proposed macro-elements and their capability to be applied for the structural assessment of masonry structures are discussed with reference to some relevant cases. Numerical and experimental validations are reported with reference to some benchmarks already investigated in the literature. The low computational cost and the easiness in the interpretation of the results make this method particularly suitable for the engineering community as well as for academic research on the seismic assessment of cultural heritage buildings.

1.2 The equivalent frame models

A widely used model for the global analysis of masonry buildings assuming an in-plane response of masonry walls is the so called ‘equivalent frame model’ (EFM). This approach can be regarded as a macro-element strategy based on the assumption that the out-of-plane response of the masonry walls is prevented and the global behaviour of the structure is ruled by the in-plane reactions of the masonry walls that can horizontally interact through diaphragms. Following the macro-element approach, each wall is idealised in several macro-portion, or structural components, to be represented by a suitable equivalent mechanical model. In the EFM it is generally assumed that in-plane damage can occur on piers and spandrels while the other masonry portion are not subjected to damage. Piers and spandrels are identified as the masonry portions between horizontally and vertically aligned openings respectively. In this macro-element approach, the masonry portions susceptible to damage are represented by equivalent nonlinear beams whose nonlinear behaviour is calibrated for describing the nonlinear response of the corresponding masonry panel. In figure 1 an example of the subdivision of a typical masonry wall in piers, spandrels and joint regions is reported; in the same figure a geometrical scheme of the corresponding equivalent frame is also represented. Under these hypothesis, the masonry portion connecting piers and spandrels, since are considered damage prevented, are regarded as rigid links connecting the equivalent beams representative piers and spandrels. This practical oriented approach leads to the definition of an equivalent frame for each plane masonry wall; the spatial connection of the plane frames by means of rigid or deformable diaphragms

allow to obtain a spatial frame model representative of the global behaviour of the overall building.

The first equivalent beam-based model can be attributed to Tomaževicˇ (1978), that introduced the so-called POR method. In this pioneering version of equivalent frame model each wall was idealised as a shear-type frame in which only the columns, representing the masonry piers, were assumed as susceptible to damage while both spandrels and connecting regions were assumed as rigid zone exempt from damage. Initially only the shear capacity of the masonry piers has been considered according to simplified elastic perfectly plastic constitutive laws. This very simple equivalent frame model strategy, although too approximate had the advantage to recognize the need to perform nonlinear analyses for masonry buildings. The POR method was lately improved by considering shear and flexural collapse mechanisms for the masonry piers leading to the POR-FLEX method (Braga & Dolce 1982, Dolce 1991). After the introduction of the POR method, some researches highlighted the need to enrich the model by introducing the possibility to identify the presence of damage also in other structural components. Taking inspiration from seismic damage scenario on unreinforced masonry buildings some research groups observed that the in-plane damage in masonry walls is mainly concentrated on piers and spandrels while the masonry portion connecting these regions are rarely subjected to significant damage. In view of this consideration the shear type model has been abandoned and a new equivalent frame models have been proposed. Calvi & Magenes (1996) introduced the SAM (Simplified Analysis of Masonry) method, then further modified by Magenes & Della Fontana (1998). In the SAM method each plane wall is represented by an equivalent frame where columns and beams represent piers and spandrels respectively. Rigid offsets describe the joint panels in which damage cannot occur. Many equivalent beam-based models (Kappos et al. 2002, P. Roca et al 2005, Penelis et al. 2006, Belmouden et al 2009) are based on the idealization of the structure as an assemblage of piers as columns and spandrels as beam elements, connected by rigid links. The main differences between these models rely on rules adopted for the definition of the equivalent frame and on the constitutive laws adopted for the description of the nonlinear behaviour of piers and spandrels. A widely used equivalent frame model is implemented in the Tremuri software (Lagomarsino et al 2013), that received several numerical and experimental validations and implements an original and versatile algorithm for the push-over analysis, suitable for assessing the nonlinear evolution of the lateral response of

3-dimensional masonry buildings, including the deterioration of the base shear for increasing lateral displacements after the attainment of peak strength. Recently some equivalent-beam based models proposed the use of distributed plasticity beam elements (Raka et al. 2015, Addessi et al 2015) leading to a better description of the nonlinear flexural behaviour being related to a fibre discretisation of the masonry.

Equivalent frame approaches represent a slender and fast solution to assess masonry buildings, whose main advantages are hereafter listed:

i. the needed degrees of freedom to model an entire building is limited, thus allowing to perform nonlinear analyses with a reasonable computational burden if compared with FE approaches;
ii. the main in-plane failure mechanisms of a masonry panel can be taken into account by means of ad hoc constitutive laws;
iii. a large part of masonry structures respects the hypotheses on which this methodology relies;
iv. the implementation of such approaches in general purposes software environments is possible.

On the other hand, these approaches present some drawbacks which limit their employability. In particular:

i. the definition of the equivalent frame is not always straightforward, especially when the distribution of the openings on the masonry walls is irregular;
ii. The geometric inconsistence between a plane masonry portion and the beam makes difficult the simulation of the interaction between reinforced concrete or steel frame structures and adjacent masonry walls. This is the case of confined masonry or infilled masonry structures.
iii. As in many macro-element approach the out-of-plane response is not taken into account.

Many works investigated and validated the EFM highlighting the difference between the approaches already proposed in the literature as well as the advantages and the limit of applicability, without claiming to be exhaustive, the interested reader can refer the recent works of Marques & Lourenço (2011), Raka et al. (2015), Quagliarini et al (2017), Siano et al. (2018).

1.3 A discrete macro-element strategy

Starting from a pioneering work in 2004 (Caliò et al. 2004) a research group of the University of Catania proposed a new macro-element method defined according to an original approach within the framework of a discrete element formulation strategy. Such an approach is based on the subdivision of the structure under consideration in several macro-portions; then, after a homogenization of the mechanical properties of the components (mortar and units), each macro-portion is regarded as an equivalent continuum whose mechanical properties can be assumed as isotropic or orthotropic depending on the masonry texture. The next step is the discretization by means of a mesh of macro-elements chosen according to the macro-portion that has to be modelled. Figure 2 reports a qualitatively subdivision of a dome by means of several macro-portions that, according to a macro-element strategy, will be represented by shell macro-elements.

In this approach each macro-element, that is not rigid, interacts with the adjacent elements through nonlinear distributed zero-thickness interfaces. The nonlinear behaviour of the structure is captured through an assemblage of macro-elements, characterized by different level of complexity according to the role played in the global model. The degrees of freedom needed to describe the macro-elements' kinematics are those strictly related to the rigid body motion plus a single degree of freedom governing the element deformability. In the following subsections a brief description of the different macro-elements introduced so far is reported.

1.3.1 The basic 2D macro-element

The basic 2D macro-element is a plane quadrangular element endowed by four degrees of freedom, Figure 3a.

The 2D macro-element, firstly proposed in 2004 (Caliò et al. 2004), has been conceived for the simulation of the nonlinear response of masonry walls in their own plane, Figure 3b. The element can be regarded as an articulated quadrilateral of rigid beams connected by four hinges, leading to a kinematics governed by four degrees of freedom only. Zero-thickness interfaces govern the interaction with the adjacent elements, while the element deformability is conveniently ruled by a single diagonal nonlinear link. The kinematics of the mechanical scheme, after a proper calibration procedure of the nonlinear links, is capable of simulating the main in-plane collapse failure modes of a masonry panel: flexural failure, diagonal shear failure and sliding shear failure (Caliò et

al., 2012a). In spite of its simplicity, the assemblage of these elements allows the simulation of the global nonlinear response of masonry buildings also in presence of openings allowing a geometric consistent simulation of the masonry walls in their own plane. Each macro-element exhibits three degrees of freedom associated with the in-plane rigid body motion, plus the additional degree of freedom, needed for the description of the in-plane shear deformability. The deformations of the interfaces are related to the relative motion between corresponding panels; therefore, no further Lagrangian parameter has to be introduced to describe their kinematics. The adopted model has the advantage of interacting with the adjacent elements along the whole perimeter, thus allowing the possibility of using different mesh discretizations as highlighted in the following paragraphs. The numerical approach has been validated by several researches (Marques and Lourenço, 2011) and it has been implemented in the software 3DMacro (Caliò et al., 2012b) currently used for research and practical applications. The geometric consistency of the elements also allows an efficient simulation of infilled frame structures, Figure 4 reports an example of infilled frame model by means of a hybrid approach in which the beams are modelled as frame elements and the infill is modelled by means of a mesh of plane macro-elements.

1.3.2 The 3D macro-element

The 2D macro-element allows the simulation of a masonry wall in its own plane but ignore the out-of-plane response. To overcome this significant restriction a third dimension and the relevant needed additional degrees of freedom have been introduced in a 3D macro-element (Pantò et al., 2017a; Pantò, 2007; Caddemi et al., 2014).

Figure 5 reports the 3D macro-element (Pantò et al., 2017a; Pantò, 2007; Caddemi et al., 2014), obtained as the extension to the space of the plane element described in the previous paragraph. The kinematics of the spatial macro-element is governed by 7 degrees-of-freedom, able to describe the in- and out-of-plane rigid body motions of the quadrilateral and the in-plane shear deformability. The interaction of the spatial macro-element with the adjacent elements or the external supports is ruled by 3D-interfaces. Each 3D-interface possesses m rows of n orthogonal (i.e. perpendicular to the planes of the interface) nonlinear links. Consequently, each interface is discretised, similarly to what is done in classical fibre models, in $m \times n$ sub-areas (Figure 5b). The 3D interfaces are endowed with additional shear-sliding springs (Figure 5a), required to control the in-plane and out-of-plane sliding mechanisms and the torsion around the axis perpendicular to the plane of the interface. The number of NLinks adopted in the 3D-

interfaces is selected according to the desired level of accuracy of the nonlinear response. A detailed description of the mechanical calibration of the spatial macro-element and its numerical and experimental validation is reported in Pantò et al 2017. This model has also been applied for the simulation of infilled frame structures accounting for the in- and the out-of-plane behaviour of infills (Pantò et al. 2018).

1.3.3 The shell macro-element for modelling curved geometry

The 3D macro-element (Pantò et al., 2017a) allows the simulation of the of in-plane and out-of-plane behaviour plane masonry walls. However Historical structures are often characterised by the presence of curved geometry structures whose role in the global and local response cannot be ignored. Aiming at modelling curved geometry a more general shell macro-element for modelling arches, vaults, domes and masonry arch bridges has been introduced. The shell macro-element is characterized by four rigid layer edges whose orientation and dimension is now associated to the shape of the element and to the thickness of the portion of structure to be modelled, Figure 6. The in-plane shear deformability is still governed by a single degree of freedom related to a diagonal spring placed along one of the diagonals of the quadrilateral. The plane interfaces rule the interaction with the adjacent elements or the external supports. However, due to the irregular geometry these interfaces are in general skew with respect to the medium plane of the element. Curved surfaces are therefore modelled under the assumption that the behaviour of a continuously curved surfaces can be adequately represented by flat macro-elements. Each quadrilateral is geometrically defined by the coordinates of its vertices, the four normal vectors to the surface and the thicknesses in these points, Figure 7.

The most significant novelties of the improved shell element can be summarized in the following features:

i. interfaces are no longer orthogonal to the plane of the element, thus allowing to follow the curved geometry of the structure;
ii. the thickness can be linearly variable at each interface;
iii. the shape of the element can be represented by a generic quadrangular element.

In spite of the complications due to the curved geometry, the model keeps the original simplicity and computational cost. Its kinematics is still ruled by seven degrees of freedom (six rigid body motion degrees of freedom and one associated with the in-plane

shear deformability). The irregular geometry implies that each link corresponds to a prismatic fiber, whose cross-sectional area varies with a parabolic trend, Figure 8.

The nonlinear sliding links are three in each interface (Figure 6b): one along the axis of the interface (in-plane sliding link) and two orthogonal to the axis and still lying on the plane of the interface (out-of-plane sliding links). The calibration strategy follows the same philosophy of the spatial regular model. Since those links have to simulate the occurrence of sliding along the bed joints, their nonlinear behavior is closely affected by friction phenomena and the yielding domain accounts for the influence of the normal force acting on the interface. In the subdivision of an arbitrary shell into flat elements, both triangular and quadrilateral elements should generally be used (see Figure 2). The triangular elements are assumed to be rigid in their own plane and are therefore characterized by six degrees of freedom only. A detailed description of the mechanical characterization of this non-trivial shell discrete element is outside the purpose of the present chapter that is oriented to a methodological description of this computationally effective approach aiming at demonstrating its suitability for practical applications devoted to the structural assessment of existing masonry structures.

1.4 The mechanical characterization strategy of the proposed macro-element approach

According to the proposed strategy each macro-element must be representative of the corresponding finite portion of masonry wall, cut out by plane sections located at the edges of the element. The formulation follows a phenomenological description of the mechanical behaviour of a masonry portion in which, the zero-thickness interfaces rule the membrane-flexural response and the shear-sliding behaviour of adjacent elements, while the in-plane shear element deformability, is related to the angular distortion of the articulated rigid quadrilateral. The mechanical characterization of the zero-thickness interfaces is here performed following a straightforward fiber calibration procedure while the shear element deformability is calibrated through a mechanical equivalence with a reference geometric-consistent continuous model. The interface nonlinear links can be distinguished as orthogonal Nlinks and shear-sliding Nlinks. In the following, the main steps needed for the calibration procedure are described with reference to each group of nonlinear links.

1.4.1 Calibration of the nonlinear links orthogonal to the interfaces

The orthogonal nonlinear links incorporate the mechanical properties of the represented element assuming masonry as an orthotropic homogeneous medium. Each orthogonal link encompasses the nonlinear behaviour of the corresponding fiber, along a given material direction, Figure 5b. With reference to a regular three-dimensional macro-element, each spring is calibrated assuming that the uniform masonry strip is a homogeneous inelastic material, which can also consider cyclic behaviour governed by fracture energy values for the tensile and compressive response, G_t and G_c, respectively, and following different post-elastic branches laws (Chácara, C. et al. 2018).

With the aim to provide an example, reference is made to a single orthotropic panel under monotonic loadings, Figure 8. In this case the flexural behaviour of the masonry panel is characterized by different mechanical properties along the two fundamental directions. E_h and E_v are the Young's moduli of the homogenized orthotropic masonry medium; σ_{ch}, σ_{th} and σ_{cv}, σ_{tv} are the corresponding compressive and tensile maximum stresses, G_{ch}, G_{th} and G_{cv}, G_{tv} are the fracture energies in compression and tension. Consistently with the here adopted fiber calibration strategy, the flexural stiffness calibration of the panel is simply obtained by assigning to each link the axial stiffness of the corresponding masonry strip. Each masonry strip is identified by its influence area and the half-dimension of the panel in the direction perpendicular to the interface, Figure 5b. The initial stiffness K, the compressive and tensile yielding strengths, f_c and f_t, and the corresponding ultimate displacements, u_c and u_t (under the simplified hypothesis of rectangular shape of the panel and linear softening) of the links relative to the horizontal and vertical interfaces are reported in Table 1 as a function of the mechanical and geometrical properties of the masonry panel.

B and H are the length and the height of the panel, λ_h and λ_v are the in-plane distances between the springs along the interfaces arranged according to the two fundamental directions, and λ_s is the out-of-plane distance between the rows of springs.

1.4.2 Calibration of the nonlinear links along the interfaces

The nonlinear links, lying along the interface and denoted as shear-sliding springs, govern the torsional and shear-sliding behaviour along the interfaces. In the discretization here adopted, one single link is considered for the in-plane model (Figure 3) while three nonlinear links have been considered for the spatial models (Figures 5 and 6), this being the minimum required to obtain the possible masonry failure modes

(Pantò et al. 2017a). A single in-plane shear-sliding spring, governing the in-plane sliding of the element along the interface is calibrated according to a rigid-plastic Mohr–Coulomb law. The out-of-plane shear deformability is ruled by two parallel springs, which take care of the out-of-plane sliding behaviour and the torsional elastic and inelastic response of the connected adjacent panels. The two out-of-plane shear-sliding nonlinear links are required to control the out-of-plane sliding mechanisms as well as the torsion around the axis perpendicular to the plane of the interface. Aiming at maintaining a simple fiber calibration approach, the out-of-plane shear deformability of each link, connecting two adjacent panels, is calibrated according to their influence volumes. Referring to two identical adjacent macro-elements, with thickness s, width B and height H, shear modulus G, cohesion c, and friction coefficient μ_s, the calibration procedure is summarized providing the main parameters that govern the mechanical behaviour of the sliding links (Table 2).

Once the elastic shear out-of-plane stiffness has been assigned, according to the formulas reported in Table 2, the relative distance d between the two out-of-plane sliding links have to be set according to an equivalence with the corresponding elastic continuum in terms of torsional behaviour (Pantò et al., 2017a). Aiming at obtaining a suitable torsional elastic calibration, although maintaining a simplified calibration strategy, the distance d between the two springs is simply obtained considering that the torsional elastic stiffness of the corresponding geometrical consistent continuous model is equivalent to that associated to the discrete system. The yielding strength of each spring is associated with the current contact area A of the interface and to the current axial force N associated with the orthogonal links of the interface.

1.4.3 Calibration of the diagonal link

The diagonal shear failure collapse of the panel is related to a single degree of freedom; this allows to associate the nonlinear response to a single diagonal nonlinear link. Many different yielding criteria can be adopted to account for the shear capacity, which is strongly dependent on the vertical compression stresses in the wall. In the elastic range, the diagonal shear spring is calibrated by imposing an energy equivalence between the articulated quadrilateral, ruled by the diagonal spring and a continuous reference elastic model. The yielding forces are associated with the limits of tensile or compressive stresses in the reference continuous model, while the post-elastic behaviour is ruled by a suitable constitutive law. A Mohr–Coulomb law or a Turnsek–

Cacovic (1970) law can generally be adopted for the calibration of the diagonal link, although any constitutive law can also be considered.

1.5 Experimental and numerical validation of the proposed macro-element strategy

In this section the capability of the proposed discrete macro-element approach to simulate the nonlinear response of masonry structures is investigated. The method is validated by comparing the numerical results with those obtained by other numerical approach or by experiments already available in the literature.

1.5.1 The 2D macro-element

The first validation is relative to the case of a single 2D macro-element which was investigated considering a comparison between the proposed approach (Pantò et al., 2015) and an equivalent frame model combined with a fiber section model recently proposed in Raka et al. (2015). The panel is restrained at its base and at its top. Initially the panel is subjected to a force controlled application of a vertical load than a displacement controlled analysis with an increasing horizontal displacement at the top of the panel is performed. The panel is characterized by the thickness t = 0.6 m, the width w = 3 m, and the height h = 2 m. The adopted mechanical properties are reported in Table 3; for this first example, the shear failure is considered inhibited.

The results are compared with those obtained by an equivalent frame approach based on a direct fiber section analysis (Raka et al 2015).

Several analyses have been performed for different levels of the axial load; in Figure 9a the ultimate bending moment of the base section is reported vs the considered axial load. The capability of the model to describe the axial-flexural response of a masonry wall section is assessed by comparing the *M-N* dominium of the base section with that obtained following the closed-form expression reported in the Italian building code (NTC, 2008). A second example of a single panel is reported in Figure 10b. The ultimate load obtained with the equivalent frame fiber model, as proposed by Raka et al 2015, and the proposed macro-element are compared when either only the flexural or only shear mechanisms are considered. The two numerical models provide very close results in terms of ultimate loads, and they are consistent with the values suggested by the Italian code (NTC, 2008)

The plane macro-element can also be adopted for modelling infilled frame structures. In the latter case a hybrid approach is applied: the surrounding frame is modelled using lumped plasticity beam–column elements while the nonlinear response of the infill is modelled by means of the plane macro-element, already described in the previous section. The frame element interacts with the masonry panels by means of nonlinear-links distribution along discrete interfaces. Each interface is constituted by *n* transversal nonlinear links and a single longitudinal nonlinear link. The flexural interaction between the panel and an adjacent beam is governed by the four degrees of freedom of the beam associated to its two ends and by the *n* internal degrees of freedom associated to the springs of the interface. For a more accurate evaluation of the nonlinear behaviour of the frame element it has been assumed that plastic hinges can occur in each sub-beam element between two nonlinear transversal links. This latter assumption provides a reliable frame element model since it is able to embed the occurrence of plastic hinges at different positions and it is consistent with the adopted level of discretization for the infill interface.

An experimental validation of the 2D macro-element, implemented in the software 3DMacro (Caliò et al., 2012b), has been provided by Marques and Lourenço (2014) with reference to three-dimensional building prototype. The experimental campaign was carried out at CISMID research center in Perù (Zavala et al., 2004) on a two storey building with irregular plan, representative to a typical family existing residential houses in Perù (Figures 11a–c). The tests were performed under quasi-static cyclic loads, applied through two actuators located at the two slabs, used to induce a constant load pattern to the structure proportional to the building height. In Figure 11b, the comparison between numerical pushover curve (dotted curve) and the experimental results is reported, while Figure 11c shows the damage scenario of the “south” wall at the last step of the analysis, a detailed comparison is reported in Marques and Lourenço (2014).

1.5.2 The 3D macro-element

An extensive numerical validation of the model on single walls with and without openings has been recently carried out in Pantò et al. (2017a) by considering masonry panels loaded out-of-plane with different geometries and boundary conditions. Applications of the model at a meso-scale for the out-of-plane behavious of masonry prototypes can be found in Cannizzaro and Lourenço (2017). The numerical applications here reported refer to a real scale simulation of a prototype building representative of

a structural typology popular in Portugal between the end of 19th century and the beginning of the 20th century. This typology, known as "Gaioleiro" buildings, corresponds to quite tall structures, usually with six stories, in which walls are made of rubble masonry and lime mortar, and the horizontal diaphragms are timber floors and roofs. A four story building with timber roofs and blind wall was investigated in the work conducted by Mendes and Lourenço (2009), Mendes (2012). Such building was built in 1:3 scale and subsequently tested on a shaking table at LNEC, Mendes et al. (2014). Details on the geometry can be found in Mendes (2012). The prototype was studied by means of an advanced FE model implemented in the software DIANA, conducting static and dynamic nonlinear analyses. The 3D macro-element method has been applied by using the software HiStrA (Caliò et al. 2015) in which the proposed macro-element strategy has been implemented. The mechanical properties here assumed are reported in Table 4 and were determined consistently with the data proposed by Mendes (2012).

A Turnsek and Cacovic (1970) yielding criterion was assumed for the diagonal shear behaviour characterised by a perfectly post-elastic behaviour till a transition drift γ_t, assumed equal to 0.6%, with a subsequent linear softening branch till the achievement of a limit drift γ_u equal to 1.5%. The numerical model consists of 704 elements (corresponding to an average mesh size equal to 1.1 m) with a total amount of degrees of freedom equal to 5568 (the FE model is characterized by 75880 degrees of freedom Mendes (2012)). The structure was initially loaded with the self weight and then subjected to horizontal mass proportional load distributions along the two main directions of the building, namely parallel and perpendicular to the façade. The target displacements for the two analyses were set according to the ultimate displacements achieved in FE model. The results reported in Figure 9 show the two capacity curves obtained from the numerical simulations. In this figure, the horizontal top displacement at a monitored node versus the base shear coefficient are reported along the horizontal and vertical axes, respectively. The monitored node corresponds to the middle point of the top wall loaded in the out-of-plane direction, whereas the base shear coefficient was computed as the base shear along the load direction normalized by the self weight. As expected, the direction parallel to the façade is weaker than the perpendicular one (peak base shear coefficient equal to 0.11 versus 0.40). Despite this, it presents a much more ductile behaviour (ultimate displacement equal to 200 mm versus 40 mm).

In Figure 13, the deformed configurations associated with the peak load and ultimate displacement are plotted with their corresponding damage patterns for the analysis in the weakest direction parallel to the main façade. Figure 13a illustrates the damage pattern associated with the peak load which is mainly characterized by the failure of spandrels in the first two stories. The damage pattern associated with the ultimate displacement is depicted in Figure 13b. In this case, it is observed that the spandrels of the upper stories present significant damage. In addition, this damage pattern was also characterized by rocking at the base of the piers.

The comparison with the FE model shows a good agreement in terms of damage patterns. In the direction parallel to the façade, the damage concentrates progressively in the spandrels, from the lower to the upper stories, leading to a final damage pattern in which the overall collapse mechanism involves all the stories.

1.5.3 The shell macro-element

The proposed macro-element approach has been implemented in the HiStrA software, specifically devoted to Historical Structures Analyses. The software allows to model typical masonry monumental structures with the aid of a graphical user interface that facilitates the input of the geometry and of the mechanical properties of the materials of the structure through the processing of a CAD drawing and the help of several generation wizard tools. In Pantò et al. (2016), with the aim to provide a numerical validation for a full scale structure, the approach has been applied to a historical basilica church, characterised by the presence of arches on masonry walls and masonry columns. A similar application can be found in Pantò et al. (2017b). In this section the capability of the shell macro-element to simulate the behaviour of typical spatial curved masonry element structures is investigated.

The applications reported in the following aim at validating the model through a comparison with experimental and numerical results. The case here reported is relative to a brick masonry spherical dome with a central hole tested in 2006 by Foraboschi (2006). The dome was subjected to an incremental vertical load along the edge of the central hole. Details on the experimental layout and on the mechanical properties can be found in Foraboschi (2006). The numerical model implemented to simulate the experimental tests consists of 544 quadrangular elements (17 along meridians and 32 along parallels) which correspond to a total number of degrees of freedom equal to

3,808. Regarding the membrane fiber discretization, a maximum distance of the orthogonal nonlinear links equal to 5 cm along the parallels and 1.5 cm through the thickness of the dome have been set, respectively. In the performed nonlinear static analysis, the model has been subjected firstly to its self-weight, then to the external vertical load applied on the annulus of quadrilateral elements sited around the hole. The mechanical properties employed in the numerical simulations, reported in Table 5, have been deduced by the simulations already reported in the literature (Milani et al., 2008; Milani and Tralli, 2012). The Elastic properties of the masonry are represented by the Young's modulus (E) and the shear Poisson's coefficient (ν). The sliding shear failure is ruled by the cohesion (c) and the friction factor (μ). The diagonal shear failure is considered elastic.

In Figure 14, the results of the nonlinear static analysis, expressed in terms of deformed shape and damage pattern at collapse, have been compared to those already available in the literature. Namely, Figure 14c reports the vertical top displacement as a function of the vertical load. The proposed model correctly predicts the initial stiffness and the ultimate load of the structure, and it is in good agreement with the available numerical results throughout all the phases of the experiment.

In Figures 14a,b, the failure mechanism and the corresponding damage scenario at the incipient collapse condition, obtained by the numerical model implemented in HiStrA (Caliò et al., 2015), are reported. More details of the comparison can be found in Caddemi et al. (2015).

1.5.4 Application to masonry arch bridges

A further structural typology to which the proposed approach has been applied is represented by masonry arch bridges. Such structures represent a large part of the railway and road infrastructures of many countries and embeds very specific structural features to which the proposed approach has been adapted, see for example the curved geometry and the three-dimensional structural response. In order to reduce the needed effort for the implementation of the numerical model of a multi-arch masonry bridge, a parametric input tool was developed considering both the complex geometry (e.g. the presence of backfill layers or the presence of tapered piers) and the automatic generation of load combinations considering the presence of a roving vehicle load (Caddemi et al. 2019). A comparison on the results obtained on a five arches railway bridge over Esino torrent (Italy) is here briefly summarized. The results obtained with the proposed

approach have been validated in the nonlinear field with those obtained with a classic nonlinear FEM approach (Lusas 2018). The adopted mechanical properties are summarized in Table 6, differentiated according to the structural components groups, considering the elastic modulus E, the shear modulus G, and the specific weight w. Tensile f_t and compressive f_c strengths of the masonry have been related to a linear softening behaviour governed by the corresponding fracture energies G_{ft} and G_{fc}. The shear diagonal behaviour has been associated to a Mohr Coulomb domain characterised by a shear strength τ_0 and a friction coefficient μ=0.5. The two numerical models, subjected to a pushdown nonlinear analysis corresponding to an anti-symmetric vehicle load arrangement, see Figure 15. The proposed approach drastically limits the required degrees of freedom (12080 versus 349362 in the FE model). Line loads have been applied to simulate the presence of vehicles, and their intensity has been magnified till the failure of the bridge. In Figure 16 a comparison in terms of both the capacity curves and the damage pattern at collapse of the two models has been reported considering as monitored displacement, for sake of conciseness, the top of second arch. A strong agreement between the two models is encountered considering the displacements of each of the five arches. The observed damage patterns of the two numerical models are similar as well, with significant vertical cracks on the first two piers and a spread damage on the arches.

1.6 Summary and conclusions

In this chapter, a numerical strategy aiming at simulating the nonlinear behaviour of masonry structures is presented. The proposed numerical model, which belongs to the framework of the simplified models, is based on a simple mechanical scheme that consists of a hinged quadrilateral, endowed with a diagonal link to govern the in-plane diagonal shear behaviour, and contouring interfaces that rule the interaction with contiguous elements.

The proposed approach appears to be a fair compromise between oversimplified models (limit analysis or equivalent frame models) and accurate models based on cumbersome strategies, which require an expert interpretation of the results. The basic model, originally conceived for the simulation of masonry walls loaded in their own plane was repeatedly upgraded, progressively increasing the structural typologies that the proposed strategy is able to model. In particular, within the scope of the numerical simu-

lation of ordinary buildings with box behaviour (the out-of-plane behaviour is considered inhibited), interaction with frames contouring a masonry panel was enabled, thus allowing the numerical simulation of both unreinforced masonry structures (URM) and infilled masonry structures (IFS).

Aiming at the numerical modeling of historical masonry structures (HMS), two further upgrades were considered. First, the out-of-plane degrees of freedom were enabled to assess the out-of-plane behaviour of masonry walls; then, a further improvement allowed simulating masonry structures with a curved geometry. Finally, by ruling the interaction between structural elements in correspondence of their intersections, full nonlinear simulations of large historical masonry constructions were performed. The progressive improvements were obtained simply extending the calibration procedure of the links according to the different peculiarities of the model at the various stages of complexity. However, the philosophy of the model was kept the same for all the considered advances of the model, that is, the calibration is always straightforward and based on the same concepts. Some simple validations of the model were presented consistently with each of the described stage. The results show that the proposed strategy appears to be reliable in all the considered cases and that it represents an original approach to the nonlinear assessment of ordinary masonry buildings, historical and monumental structures.

1.7 Ackowledgements

The research is supported by the AGM for CuHe project (ARS01_00697). PNR 2015-2020. Area di Specializzazione “CULTURAL HERITAGE”. CUP E66C18000380005.

1.8 References

Addessi, D, Liberatore, Masiani, R 2015 ‘Force-based beam finite element (FE) for the pushover analysis of masonry buildings’, *International Journal of Architectural Heritage*, vol. 9, no. 3, pp. 231–243.

Anthoine, A 1997, 'Homogenisation of periodic masonry: plane stress, generalised plane strain or 3D modelling?' *Communications in Numerical Methods in Engineering,* vol. 13, pp. 319–326, doi:10.1002/(SICI)1099-0887(199705)13:5<319::AID-CNM55>3.3.CO;2-J.

Araujo, A, Lourenço, PB, Oliveira, D, & Leite, J 2012, 'Seismic assessment of St James Church by means of pushover analysis – before and after the New Zealand earthquake' *Open Civil Engineering Journal, vol.* 6, pp. 160–172, doi:10.2174/1874149501206010160.

Asteris, PG, Antoniou, ST, Sophianopoulos, D, & Chrysostomou, CZ 2011, 'Mathematical macromodeling of infilled frames: state of the art' *Journal of Structural Engineering, vol.* 137, pp. 1508–1517, doi:10.1061/(ASCE)ST.1943-541X.0000384.

Asteris, PG, Chronopoulos, MP, Chrysostomou, CZ, Varum, H, Plevris, V, Kyriakides, N, & Silva, V 2014, 'Seismic vulnerability assessment of historical masonry structural systems' *Engineering Structures,* vol. 62-63, pp. 118–134, doi:10.1016/j.engstruct.2014.01.031.

Barbieri, G, Biolzi, L, Bocciarelli, M, Fregonese, L, & Frigeri, A 2013, 'Assessing the seismic vulnerability of a historical building' *Engineering Structures, vol.* 57, pp. 523–535, doi:10.1016/j.engstruct.2013.09.045.

Belmouden, Y, Lestuzzi, P 2009 , 'An equivalent frame model for seismic analysis of masonry and reinforced concrete buildings' *Construction and Building Materials*, vol. 23, no. 1, pp. 40–53.

Berto, L, Saetta, A, Scotta, R, & Vitaliani, R 2002, 'Orthotropic damage model for masonry structures' *International Journal of Numerical Methods in Engineering, vol.* 55, pp. 127–157, doi:10.1002/nme.495.

Betti, M, & Vignoli, A 2008, 'Assessment of seismic resistance of a basilica-type church under earthquake loading: modelling and analysis' *Advances in Engineering Software,* vol. 39, pp. 258–283, doi:10.1016/j.advengsoft.2007.01.004.

Betti, M, & Vignoli, A 2011, 'Numerical assessment of the static and seismic behaviour of the basilica of Santa Maria all'Impruneta (Italy)' *Constructions and Building Materials, vol.* 25, pp. 4308–4324, doi:10.1016/j.conbuildmat.2010.12.028.

Braga, F, & Dolce, M 1982, 'Un metodo per l'analisi di edifici multipiano in muratura antisismici, Proc. of the 6th I.B.MA.C - International Brick Masonry Conference, Rome.

Brenchich, G, Gambarotta, L, & Lagomarsino, S 1998, 'A macro-element approach to the three-dimensional seismic analysis of masonry buildings', in *Proceedings of 11th European Conference on Earthquake Engineering* (Paris, Rotterdam: A. A. Balkema), 602.

Caddemi S, Caliò I, Cannizzaro F, Occhipinti, G, & Pantò, B 2015, 'A parsimonious discrete model for the seismic assessment of monumental structures', in *Proceedings of the Fifteenth International Conference on Civil, Structural and Environmental Engineering Computing*, eds J. Kruis, Y. Tsompanakis, and B. H. V. Topping (Stirlingshire, UK: Civil-Comp Press), Paper 82.

Caddemi, S, Caliò, I, Cannizzaro, F, & Pantò, B 2013, 'A new computational strategy for the seismic assessment of infilled frame structures', in *Proceedings of the Fourteenth International Conference on Civil, Structural and Environmental Engineering Computing*, eds B. H. V. Topping and P. Iványi (Stirlingshire, UK: Civil-Comp Press), Paper 77.

Caddemi, S, Caliò, I, Cannizzaro, F, & Pantò, B 2014, 'The seismic assessment of historical masonry structures', in *Proceedings of the Twelfth International Conference on Computational Structures Technology*, eds B. H. V. Topping and P. Iványi (Stirlingshire, UK: Civil-Comp Press), Paper 78.

Caddemi, S, Caliò, I, Cannizzaro, F, Chacara, C, D'Urso, D, Liseni, S, Lourenço, PB, Occhipinti, G, Pantò, B, & Rapicavoli, D 2018, 'An original discrete macro-element method for the analysis of historical structures', in *Proceedings of the 16th European Conference on Earthquake Engineering,* Thessaloniki (Greece), 18-21 June 2018.

Caddemi, S, Caliò, I, Cannizzaro, C, D'Urso, D, Occhipinti, G, Pantò, B, & Rapicavoli, D 2019, '3D Discrete Macro-Modelling Approach for Masonry Arch Bridges', in *IABSE Symposium 2019,* Guimarães (Portugal), 27-29 March 2019.

Caliò, I, Marletta, M, & Pantò, B 2004, 'Un semplice macro-elemento per la valutazione della vulnerabilità sismica di edifici in muratura', *atti dell'XI congresso nazionale l'Ingegneria Sismica in Italia,* Genova 2004. (in Italian)

Caliò, I, Cannizzaro, F, D'Amore, E, Marletta, M, & Pantò, B 2008, 'A new discrete-element approach for the assessment of the seismic resistance of composite reinforced concrete-masonry buildings', in *AIP Conference Proceedings*, 1020 (PART 1); 2008 Jun 24–27; Reggio Calabria, pp. 832–839.

Calió, I, Cannizzaro, F, & Marletta, M 2010, 'A discrete element for modeling masonry vaults' *Advanced Materials Research*, vol. 133-134, pp. 447–452, doi:10.4028/www.scientific.net/AMR.133-134.447.

Caliò, I, Cannizzaro, F, Pantò, B, & Rapicavoli, D 2015, 'HiStrA (historical structure analysis)', in HISTRA s.r.l (Catania, Italy). Release 17.2.3; April 2015. Available at: http://www.grupposismica.it

Caliò, I, Marletta, M, & Pantò, B 2005, 'A simplified model for the evaluation of the seismic behaviour of masonry buildings', in *Proceedings of the Tenth International Conference on Civil, Structural and Environmental Engineering Computing*, ed. B. H. V. Topping (Stirlingshire: Civil-Comp Press), 195.

Caliò, I, Marletta, M, & Pantò, B 2012a, 'A new discrete element model for the evaluation of the seismic behaviour of unreinforced masonry buildings' *Engineering Structures,* vol. 40, pp. 327–338, doi:10.1016/j.engstruct.2012.02.039.

Caliò, I, Cannizzaro, F, Marletta, M, & Pantò, B 2012b, '3DMacro: A 3D Computer Program for the Seismic Assessment of Masonry Buildings', Catania, Italy: Gruppo Sismica s.r.l.

Caliò, I, & Pantò, B 2014, A macro-element modelling approach of infilled frame structures', *Computers & Structures, vol.* 143, pp. 91–107, doi:10.1016/j.compstruc.2014.07.008.

Cannizzaro, F 2010, 'The Seismic Behaviour of Historical Buildings: A Macro-Element Approach' PhD Thesis in Structural Engineering, in Italian, University of Catania.

Cannizzaro, F, & Lourenço, PB 2017, 'Simulation of shake table tests on out-of-plane masonry buildings. Part (VI): discrete element approach', *International Journal of Architectural Heritage*, vol. 11, pp. 125–142.

Cannizzaro, F, Pantò, B, Caddemi, S, & Caliò, I 2018, 'A Discrete Macro-Element Method (DMEM) for the nonlinear structural assessment of masonry arches', *Engineering Structures,* vol. 168, pp. 243-256, doi: 10.1016/j.engstruct.2018.04.006.

Casolo, S, & Peña, F 2007, 'Rigid element model for in-plane dynamics of masonry walls considering hysteretic behaviour and damage', *Earthquake Engineering and Structural Dynamics,* vol. 36, pp. 1029–1048, doi:10.1002/eqe.670.

Casolo, S, & Sanjust, CA 2009, 'Seismic analysis and strengthening design of a masonry monument by a rigid body spring model: the "Maniace Castle" of Syracuse', *Engineering Struct*ures, vol. 31, pp. 1447–1459, doi:10.1016/j.engstruct.2009.02.030.

Chácara, C, Cannizzaro, F, Pantò, B, Caliò, I, Lourenço, PB 2018, 'Assessment of the dynamic response of unreinforced masonry structures using a macro-element modeling approach', *Earthquake Engineering & Structural Dynamics,* vol. 47(12), pp. 2426-2446.

Chen, SY, Moon, FL, Yi, T 2008, 'A macroelement for the nonlinear analysis of in-plane unreinforced masonry piers', *Engineering Structures*, vol. 30(8), pp. 2242-2252, doi:10.1016/j.engstruct.2007.12.001.

FEA ltd, LUSAS - Theory Manuals, Lusas Version 16.0, 2018.

M. Dolce, "Schematizzazione e modellazione degli edifici in muratura soggetti ad azioni sismiche," L'Industria delle costruzioni, vol. 25, no. 242, pp. 44–57, 1991. (in italian)

Foraboschi, P 2006, 'Masonry structures externally reinforced with FRP strips: tests at the collapse [in Italian]', in *Proceedings of I Convegno Nazionale Sperimentazioni su Materiali e Strutture* (Venice).

Gambarotta, L, & Lagomarsino, S 1997, 'Damage models for the seismic response of brick masonry shear walls. Part II: the continuum model and its applications', *Earthqake Engineering and Structural Dynamics,* vol. 26, pp. 441–462, doi:10.1002/(SICI) 1096-9845(199704)26:4<423::AID-EQE650>3.0.CO;2-#.

Hilsdorf, HK 1969, "Investigation into the failure mechanism of brick masonry loaded in axial compression" *Designing, engineering and constructing with masonry products,* Gulf Publishing Company, pp. 34–41.

Kappos, AJ, Penelis, GG, & Drakopoulos, CG 2002, 'Evaluation of simplified models for lateral load analysis of unreinforced masonry buildings', *Journal of Structural Engineering,* vol. 128, pp. 890–897, doi:10.1061/(ASCE)0733-9445(2002)128:7(890).

Lagomarsino, S., Penna, A., Galasco, A., and Cattari, S. (2013). TREMURI program: an equivalent frame model for the nonlinear seismic analysis of masonry buildings. Eng. Struct. 56, 1787–1799. doi:10.1016/j.engstruct.2013.08.002.

Lofti, HR, & Shing, PB 1994, 'Interface model applied to fracture of masonry structures', *Journal of Structural Engineering,* vol. 120, pp. 63–80, doi:10.1061/(ASCE)0733-9445 (1994)120:1(63).

Lourenço, PB 2002, 'Computations on historic masonry structures', *Progress in Structural Engineering and Materials*, vol. 4, pp. 301–319. doi:10.1002/pse.120.

Lourenço, PB, Nuno Mendes, AT, & Ramos, LF 2012, 'Seismic performance of the St. George of the Latins church: lessons learned from studying masonry ruins', *Engineering Structures,* vol. 40, pp. 501–518, doi:10.1016/j.engstruct.2012.03.003.

Lourenço, PB, & Rots, JG 1997, 'A multi-surface interface model for the analysis of masonry structures' *Journal of Engineering Mech*anics, vol. 123, pp. 660–668. doi:10.1061/(ASCE)0733-9399(1997)123:7(660).

Lourenço, PB, Rots, JG, & Blaauwendraad, J 1998, 'Continuum model for masonry: parameter estimation and validation', *Journal of Structural Eng*ineering, vol. 124, pp. 642–652, doi:10.1061/(ASCE)0733-9445(1998)124:6(642).

Macorini, L, & Izzuddin, BA 2011, 'A non-linear interface element for 3D mesoscale analysis of brick-masonry structures', *International Journal of Numerical Methods in Eng*ineering, vol. 85, pp. 1584–1608, doi:10.1002/nme.3046.

Magenes, G, & Della Fontana, A 1998, 'Simplified nonlinear seismic analysis of masonry buildings', *British Masonry Society Proceedings*, no. 8, pp. 190–195.

Marques, R, & Lourenço, PB 2011, 'Possibilities and comparison of structural component models for the seismic assessment of modern unreinforced masonry buildings' *Computers & Structures*. vol. 89, pp. 2079–2091, doi:10.1016/j.compstruc.2011.05.021.

Marques, R, & Lourenço, PB 2014, 'Unreinforced and confined masonry buildings in seismic regions: validation of macro-element models and cost analysis', *Engineering Struct*ures, vol. 64, pp. 52–67, doi:10.1016/j.engstruct.2014.01.014.

Mele, E, De Luca, A, & Giordano, A 2003, 'Modelling and analysis of a basilica under earthquake loading', *Journal of Cultural Herit*age, vol. 4, pp. 355–367, doi:10.1016/j.culher.2003.03.002.

Mendes N, & Lourenço PB 2009, 'Seismic assessment of masonry "Gaioleiro" buildings in Lisbon, Portugal' *Journal of Earthquake Engineering,* vol. 14, pp. 80-101.

Mendes N 2012 'Seismic assessment of ancient masonry buildings: shaking table tests and numerical analysis' PhD Thesis in Civil Engineering, University of Minho.

Mendes N, Lourenço PB, & Campos-Costa A 2014, ‘Shaking table testing of an existing masonry building: assessment and improvement of the seismic performance’ *Earthquake Engineering and Structural Dynamics*, vol. 43(2), pp. 247-266.

Milani, E, Milani, G, & Tralli, A 2008, 'Limit analysis of masonry vaults by means of curved shell finite elements and homogenization', *International Journal of Solids and Struct*ures, vol. 45, pp. 5258–5288, doi:10.1016/j.ijsolstr.2008.05.019.

Milani, G, & Tralli, A 2012, 'A simple meso-macro model based on SQP for the non-linear analysis of masonry double curvature structures', *International Journal of Solids and Struct*ures, vol. 46, pp. 808–834, doi:10.1016/j.ijsolstr.2011.12.001.

Milani, G, & Valente, M 2015, 'Failure analysis of seven masonry churches severely damaged during the 2012 Emilia-Romagna (Italy) earthquake: non-linear dynamic analyses vs conventional static approaches', *Engineering Failure Anal*ysis, vol. 54, pp. 13–56, doi:10.1016/j.engfailanal.2015.03.016.

NTC 2008, Decreto Ministeriale. Norme tecniche per le costruzioni. Ministry of Infrastructures and Transportations. G.U. S.O. n.30 on 4/2/2008;2008 [in Italian].

Pantò, B 2007, 'The Seismic Modeling of Masonry Structure, An Innovative Macro-Element Approach' PhD Thesis in Structural Engineering, in Italian. Catania: University of Catania.

Pantò, B, Cannizzaro, F, Caddemi, S, & Caliò, I 2016, '3D macro-element modelling approach for seismic assessment of historical masonry churches', *Advances in Engineering Softw*are, vol. 97, pp. 40–59, doi:10.1016/j.advengsoft.2016.02.009.

Pantò, B, Cannizzaro, F, Caliò, I, & Lourenço, PB 2017a, 'Numerical and experimental validation of a 3D macro-model element method for the in-plane and out-of-plane behaviour of unreinforced masonry walls', *International Journal of Architectural Herit*age, vol. 11, no. 7, pp. 946-964, doi:10.1080/15583058.2017.1325539.

Pantò, B, Giresini, L, Sassu, M, & Caliò, I 2017b, 'Non-linear modeling of masonry churches through a discrete macro-element approach', *Earthquakes and Struct*ures, vol. 12, pp. 223–236, doi:10.12989/eas.2017.12.2.223.

Pantò, B, Raka, E, Cannizzaro, F, Camata, G, Caddemi, S, Spacone, E, & Caliò, I 2015, 'Numerical macro-modeling of unreinforced masonry structures: a critical appraisal', in *Proceedings of the Fifteenth International Conference on Civil, Structural*

and Environmental Engineering Computing, eds B. H. V.Topping and P. Iványi (Stirlingshire: Civil-Comp Press).

Pantò, B, Caliò, I, Lourenço, PB 2018 A 3D discrete macro-element for modelling the out-of-plane behaviour of infilled frame structures *Engineering Structures*, vol. 175, pp. 371-385, doi: 10.1016/j.engstruct.2018.08.022.

G. G. Penelis, GG 2006, 'An efficient approach for pushover analysis of unreinforced masonry (URM) structures' *Journal of Earthquake Engineering*, vol. 10, no. 03, pp. 359–379.

Quagliarini, E, Maracchini, G, Clementi, F, 2017 'Uses and limits of the Equivalent Frame Model on existing unreinforced masonry buildings for assessing their seismic risk: A review', *Journal of Building Engineering*, vol. 10, pp. 166-182, doi:10.1016/j.jobe. 2017.03.004.

Raka, E, Spacone, E, Sepe, V, & Camata, G 2015, 'Advanced frame element for seismic analysis of masonry structures: model formulation and validation', *Earthquake Engineering and Structural D*ynamics, vol. 44, pp. 2489–2506, doi:10.1002/eqe.2594.

Roca, P, Molins, C, & Marí, AR, 2005 "Strength capacity of masonry wall structures by the equivalent frame method," Journal of structural engineering, vol. 131, no. 10, pp. 1601–1610.

Siano, R, Roca, P, Camata, G, Pelà, L, Sepe, V, Spacone, E, Petracca, M 2018 'Numerical investigation of non-linear equivalent-frame models for regular masonry walls *Engineering Structures*, 173, pp. 512-529.

Tomazevic, M 1978, 'The computer program POR: institute for testing and research in materials and structures' ZRMK. Ljubljana, Slovenia.

Turnšek, V, & Čačovič, F 1970, 'Some experimental results on the strength of brick masonry walls', in *Proceedings of the 2nd International Brick & Block Masonry Conference* (Stoke-on-Trent), pp. 149–156.

Valente, M, & Milani, G 2016, 'Seismic assessment of historical masonry towers by means of simplified approaches and standard FEM' *Construction and Building Materials,* vol. 108, pp. 74-104, doi: 10.1016/j.conbuildmat.2016.01.025.

Zavala, C, Honma, C, Gibu, P, Gallardo, J, & Huaco, G 2004, 'Full scale on line test on two story masonry building using handmade bricks', in *Proceedings of the 13th World Conference on Earthquake Engineering* (Vancouver), 2885.

Table 1. Mechanical calibration of the orthogonal *Nlinks* for a rectangular panel

Direction	K	f_c	f_t	u_c	u_t
Horizontal	$K_h = 2\frac{E_h \lambda_h \lambda_s}{B}$	$f_{ch} = \sigma_{ch} \lambda_h \lambda_s$	$f_{th} = \sigma_{th} \lambda_h \lambda_s$	$u_{ch} = 2\frac{G_{ch}}{\sigma_{ch}}$	$u_{th} = 2\frac{G_{th}}{\sigma_{th}}$
Vertical	$K_v = 2\frac{E_v \lambda_v \lambda_s}{H}$	$f_{cv} = \sigma_{cv} \lambda_v \lambda_s$	$f_{tv} = \sigma_{tv} \lambda_v \lambda_s$	$u_{cv} = 2\frac{G_{cv}}{\sigma_{cv}}$	$u_{t2} = 2\frac{G_{tv}}{\sigma_{tv}}$

Table 2. Mechanical calibration of the shear sliding Nlinks for a rectangular panel

Direction	k_S	d	f_{sy}
In-plane	∞	-	$f_{sy} = \left(c + \mu_s N\right) A$
Out-of-plane	$k_s = \frac{1}{2}\frac{GBs}{H}$	$d = 2s\sqrt{\frac{1}{3} - 0,21\frac{s}{B}\left(1 - \frac{s^4}{12B^4}\right)}$	$f_{sy} = \frac{1}{2}\left(c + \mu_s N\right) A$

Table 3. Mechanical properties adopted for the masonry

G [MPa]	E [MPa]	ρ [kN/m^3]	σ_c [MPa]	σ_t [MPa]	f_{v0}
230	870	19	1.0	0.1	0.4

Table 4. Mechanical properties adopted in the numerical model.

E [MPa]	σ_t [MPa]	G_t [N/mm]	σ_c [MPa]	G_c [N/mm]	G [MPa]	γ_t [%]	γ_u [%]
1000	0.1	0.05	100	1.6	417	0.6	1.5

Table 5. Mechanical properties adopted in the numerical model.

E [MPa]	σ_t [MPa]	σ_c [MPa]	c [MPa]	μ	ν	γ [kN/m^3]
850	0.07	1.9	0.12	0.37	0.25	19

Table 6. Mechanical properties adopted for the masonry bridge

Elements	f_m [MPa]	τ_0 [MPa]	E [MPa]	G [MPa]	f_t [MPa]	G_{ft} [MPa]	G_{fc} [MPa]	w [kN/m^3]
Abutment, pier, spandrel wall	5.8	0.4	2060	860	0.12	0.02	100	22
Masonry arches	2.6	0.3	1200	500	0.12	0.02	100	18
Backing, fill material, ballast	1.1	0.05	700	290	0.05	∞	100	19

Captions

Figure 1. Equivalent frame modelling strategy. (1) masonry wall geometrical layout; (2) identification of piers, spandrels and regions assumed as rigid; (3) frame model superimposed to the wall geometry; (4) equivalent frame model

Figure 2. Subdivision of a dome in macro-portion to be represented by macro-elements.

Figure 3. The 2D macro-element and its mechanical scheme. (a) initial undeformed configuration (b) deformed configuration.

Figure 4. Typical macro-element discretization of an infilled frame in presence of a central door opening.

Figure 5. 3D macro-element. (a) simplified mechanical scheme; (b) a typical fiber discretization of the element.

Figure 6. Shell macro-element. (a) the orthogonal links of the interfaces; (b) the longitudinal and the diagonal links.

Figure 7. (a) Curved portion of masonry structures and (b) its flat discrete element representation.

Figure 8. Fiber discretization of the shell macro-element.

Figure 9. Mechanical characterization of an orthotropic masonry panel: (a) constitutive laws and (b) calibration of the orthogonal Nlinks (Pantò et al., 2017a).

Figure 10. Interaction diagrams: (a) M-N and (b) V-N (Pantò et al., 2015).

Figure 11. Experimental validation of the 2D macro-element for a prototype building (Marques and Lourenço, 2014): (a) numerical model, (b) comparison in terms of capacity curve and (c) damage scenario at collapse of the south wall.

Figure 12. Numerical validation of the 3D macro-element through a comparison with FE results for a Gaioleiro prototype buildings (Caddemi et al, 2018). Capacity curves along the directions (a) parallel and (b) orthogonal to the façade.

Figure 13. Damage pattern at (a) the peak load and (b) at collapse for the analyses along the direction parallel to the façade (Caddemi et al, 2018).

Figure 14. Hemispherical dome (Caddemi et al., 2015): (a) failure mechanism represented in half dome (b) Damage inelastic distribution expressed in gray scale (c) load displacement curves.

Figure 15. Railway bridge (Caddemi et al., 2019): (a) layout of the applied loads and numerical models according to (b) proposed and (c) the FE approaches.

Figure 16. Comparison in terms of (a) capacity curves and damage pattern at collapse according to (b) proposed and (c) the FE approaches.

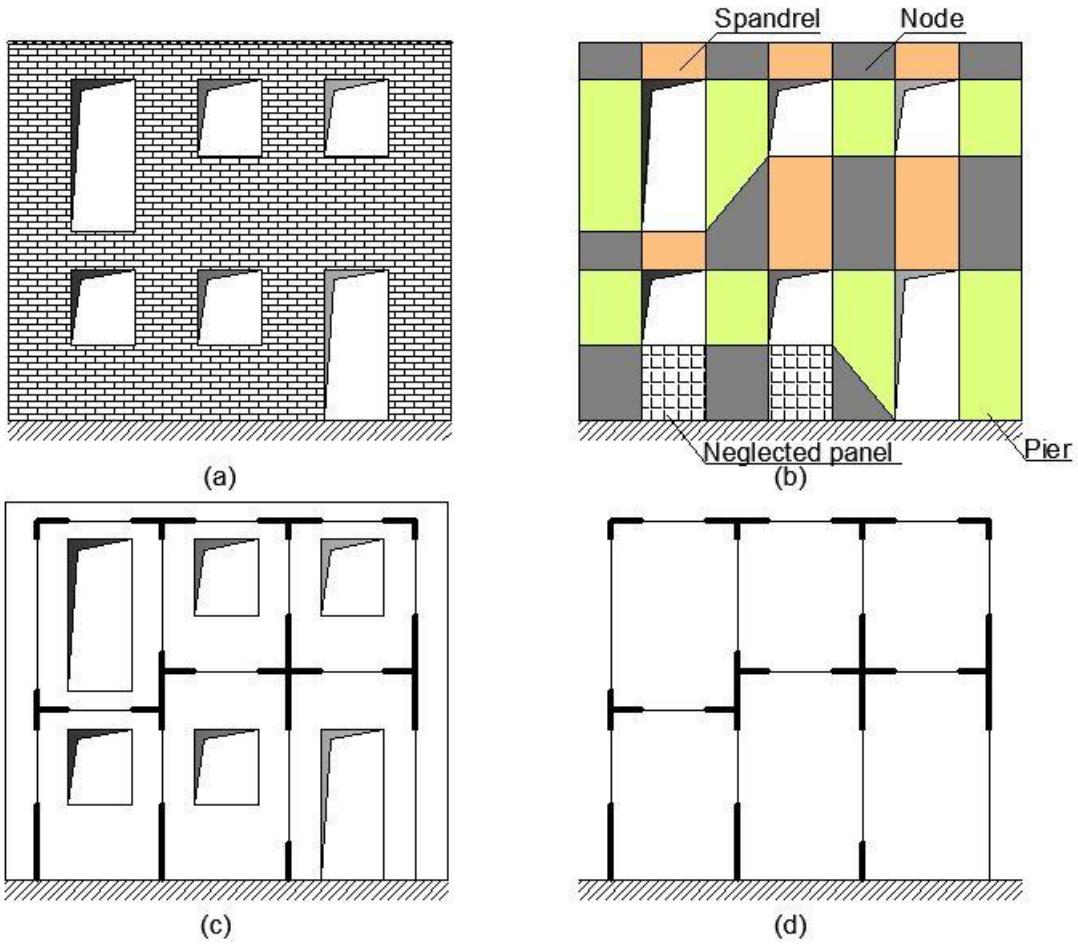

Figure 1. Equivalent frame modelling strategy. (1) masonry wall geometrical layout; (2) identification of piers, spandrels and regions assumed as rigid; (3) frame model superimposed to the wall geometry; (4) equivalent frame model

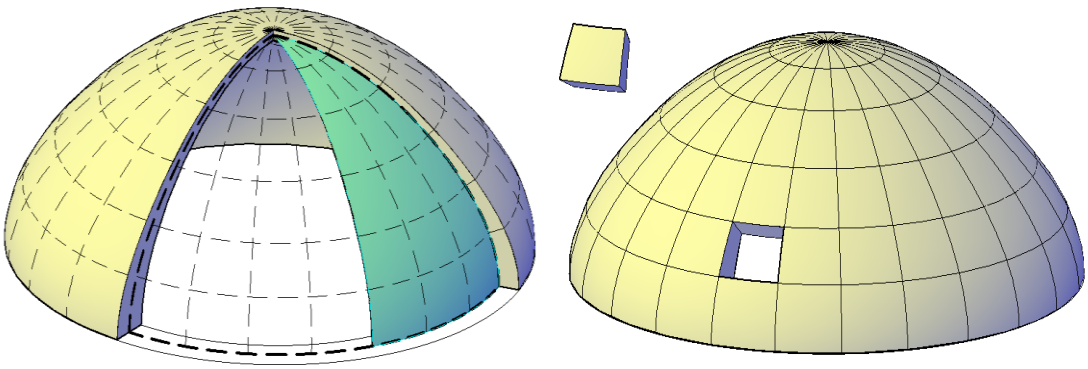

Figure 2. Subdivision of a dome in macro-portion to be represented by macro-elements.

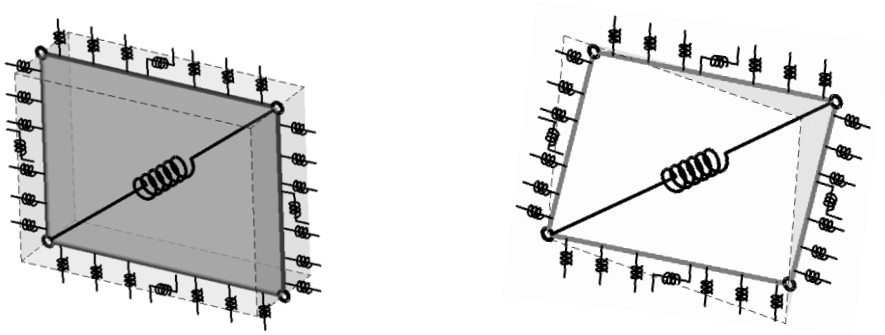

(a) (b)

Figure 3. The 2D macro-element and its mechanical scheme. (a) initial undeformed configuration (b) deformed configuration.

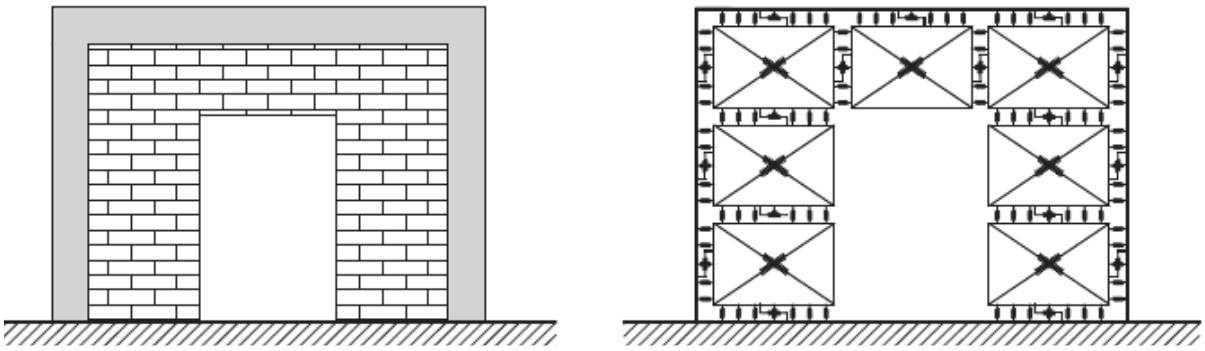

Figure 4. Typical macro-element discretization of an infilled frame in presence of a central door opening.

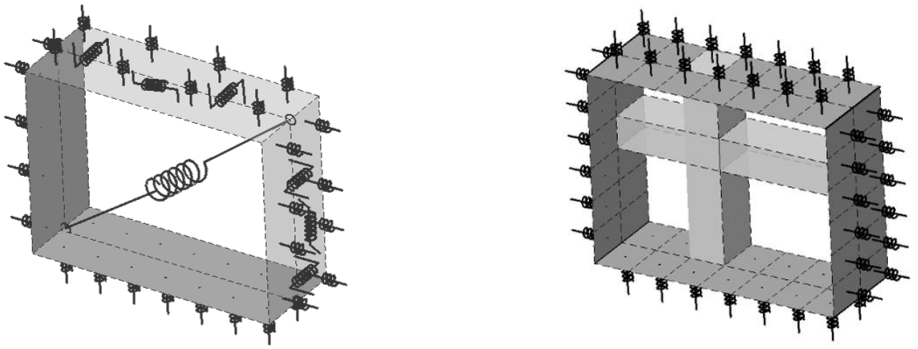

(a) (b)

Figure 5. 3D macro-element. (a) simplified mechanical scheme; (b) a typical fiber discretization of the element.

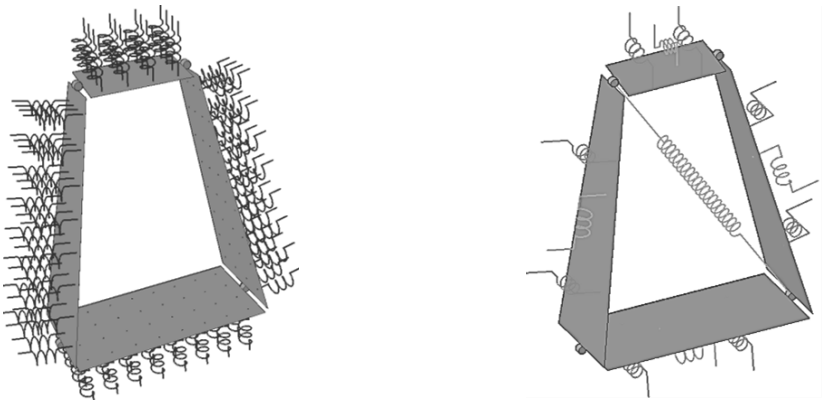

(a) (b)

Figure 6. Shell macro-element. (a) the orthogonal links of the interfaces; (b) the longitudinal and the diagonal links.

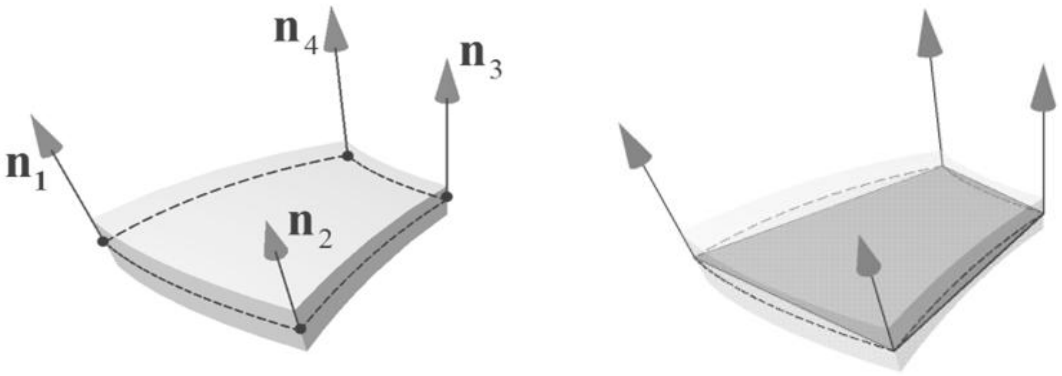

(a) (b)

Figure 7. (a) Curved portion of masonry structures and (b) its flat discrete element representation.

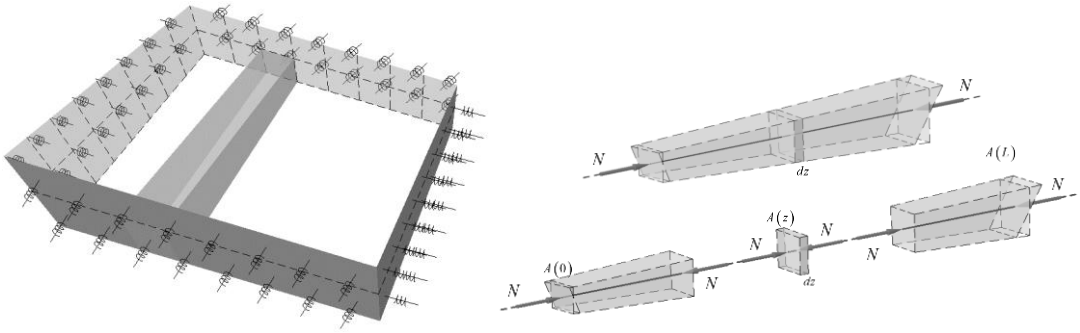

Figure 8. Fiber discretization of the shell macro-element.

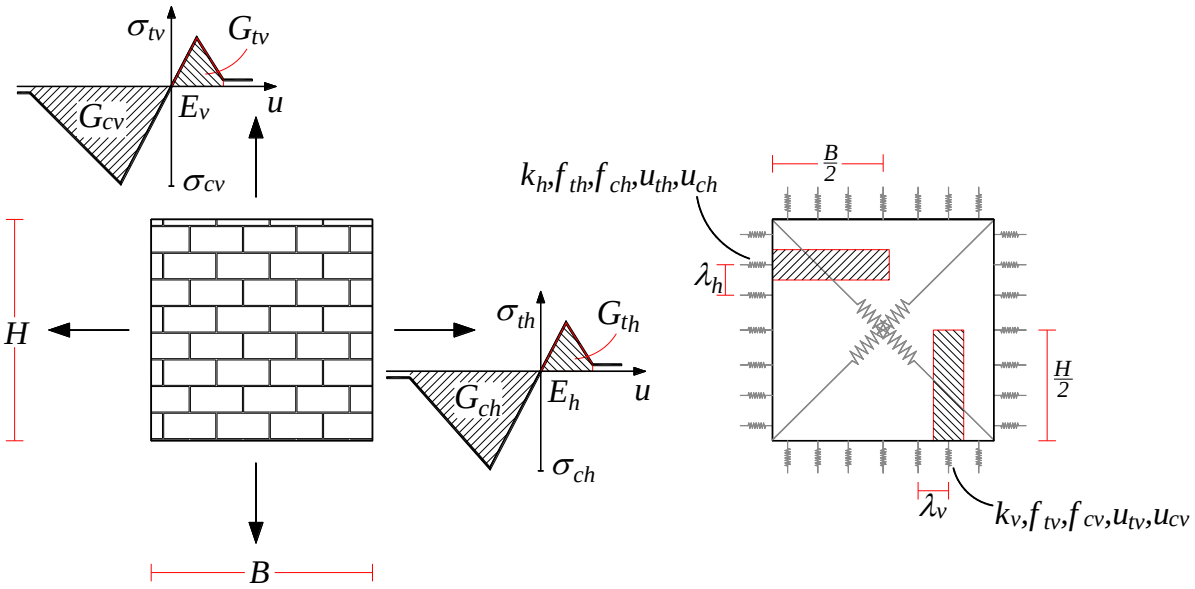

Figure 9. Mechanical characterization of an orthotropic masonry panel: (a) constitutive laws and (b) calibration of the orthogonal Nlinks (Pantò et al., 2017a).

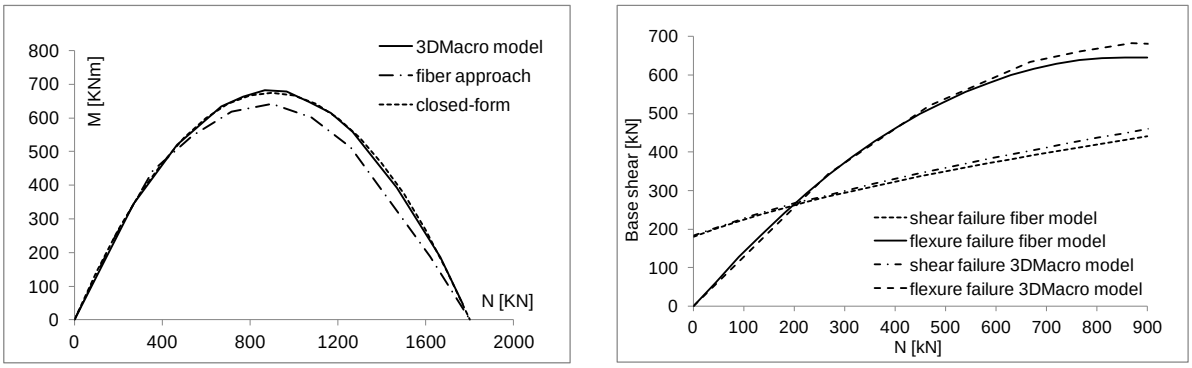

(a) (b)

Figure 10. Interaction diagrams: (a) M-N and (b) V-N (Pantò et al., 2015).

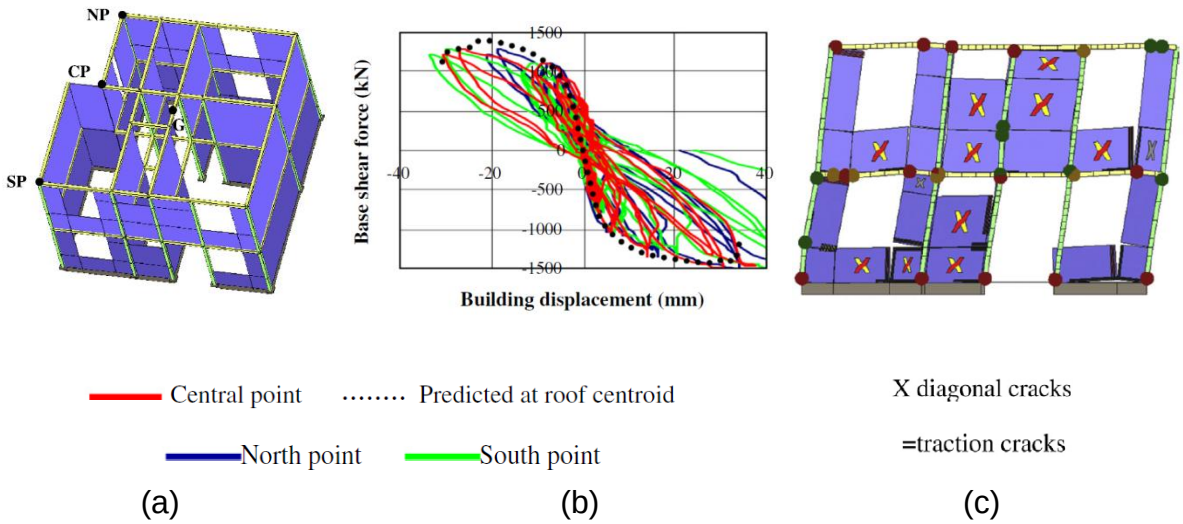

Figure 11. Experimental validation of the 2D macro-element for a prototype building (Marques and Lourenço, 2014): (a) numerical model, (b) comparison in terms of capacity curve and (c) damage scenario at collapse of the south wall.

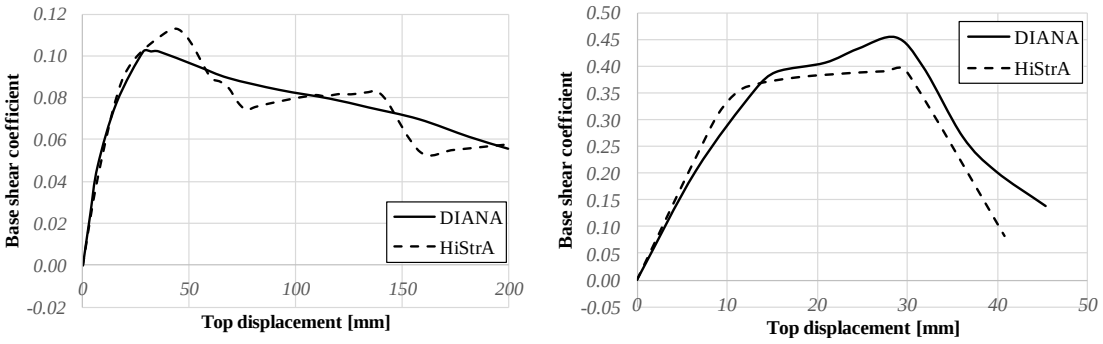

(a) (b)

Figure 12. Numerical validation of the 3D macro-element through a comparison with FE results for a Gaioleiro prototype buildings (Caddemi et al, 2018). Capacity curves along the directions (a) parallel and (b) orthogonal to the façade.

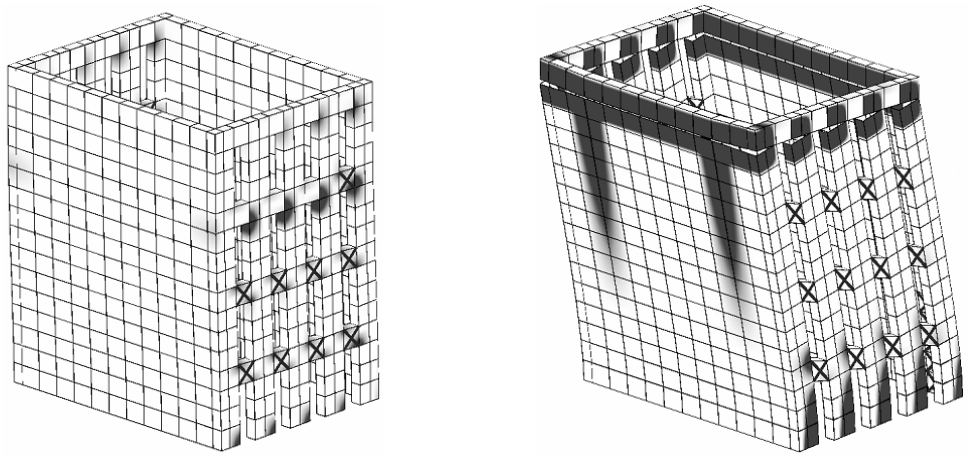

(a) (b)

Figure 13. Damage pattern at (a) the peak load and (b) at collapse for the analyses along the direction parallel to the façade (Caddemi et al, 2018).

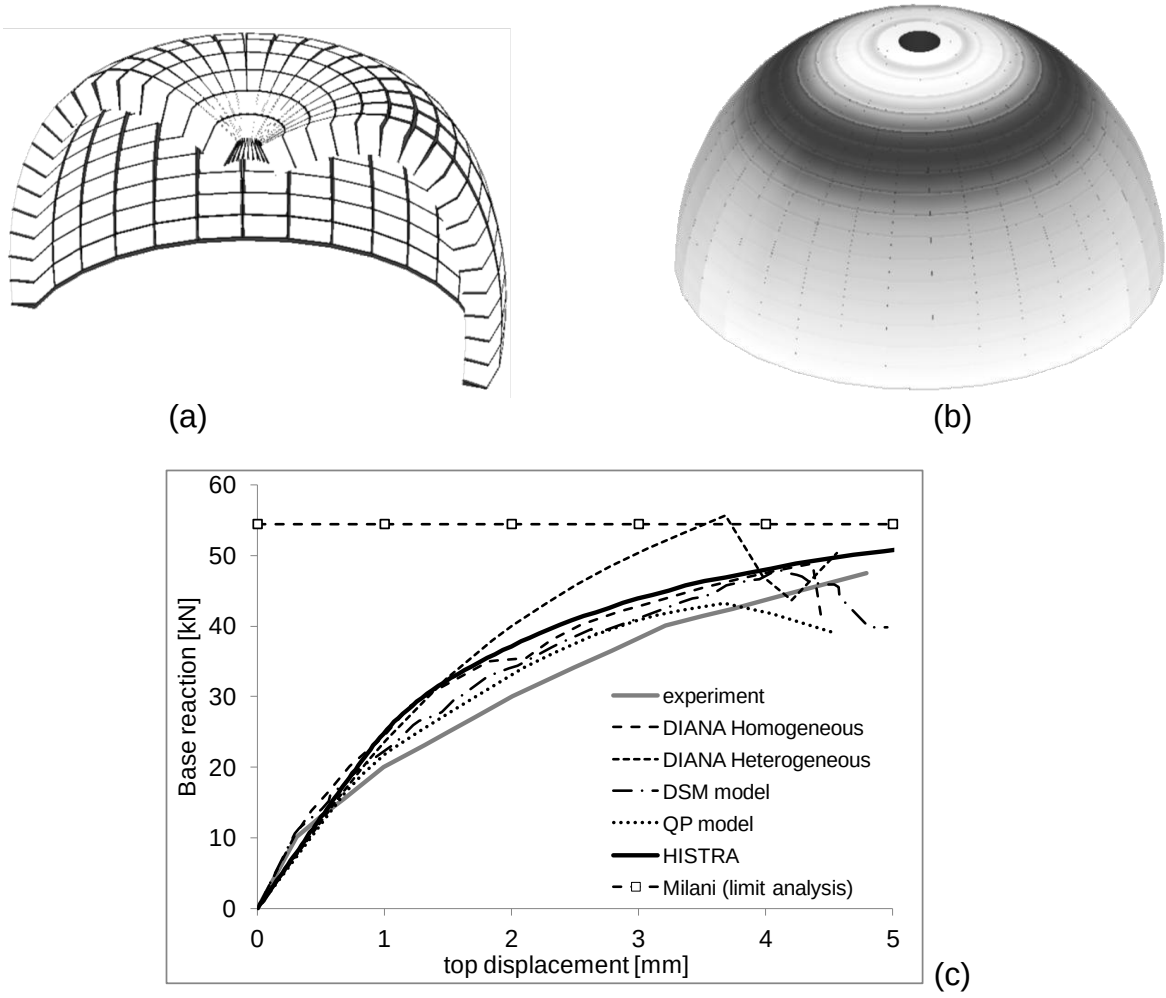

Figure 14. Hemispherical dome (Caddemi et al., 2015): (a) failure mechanism represented in half dome (b) Damage inelastic distribution expressed in grey scale (c) load displacement curves.

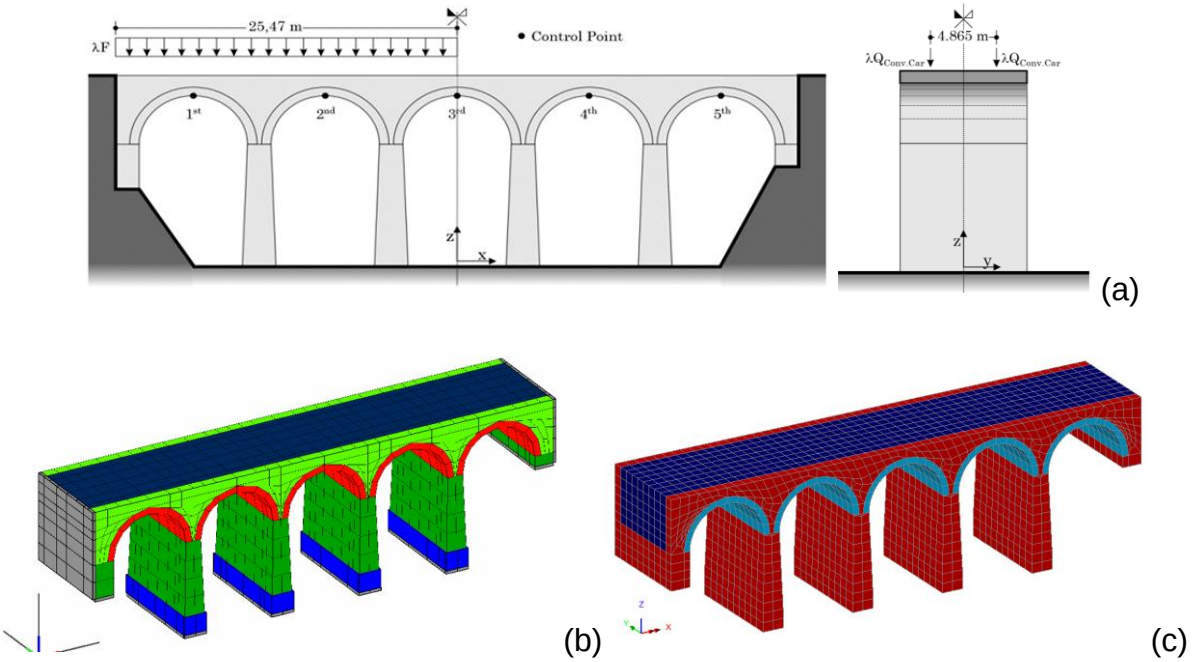

Figure 15. Railway bridge (Caddemi et al., 2019): (a) layout of the applied loads and numerical models according to (b) proposed and (c) the FE approaches.

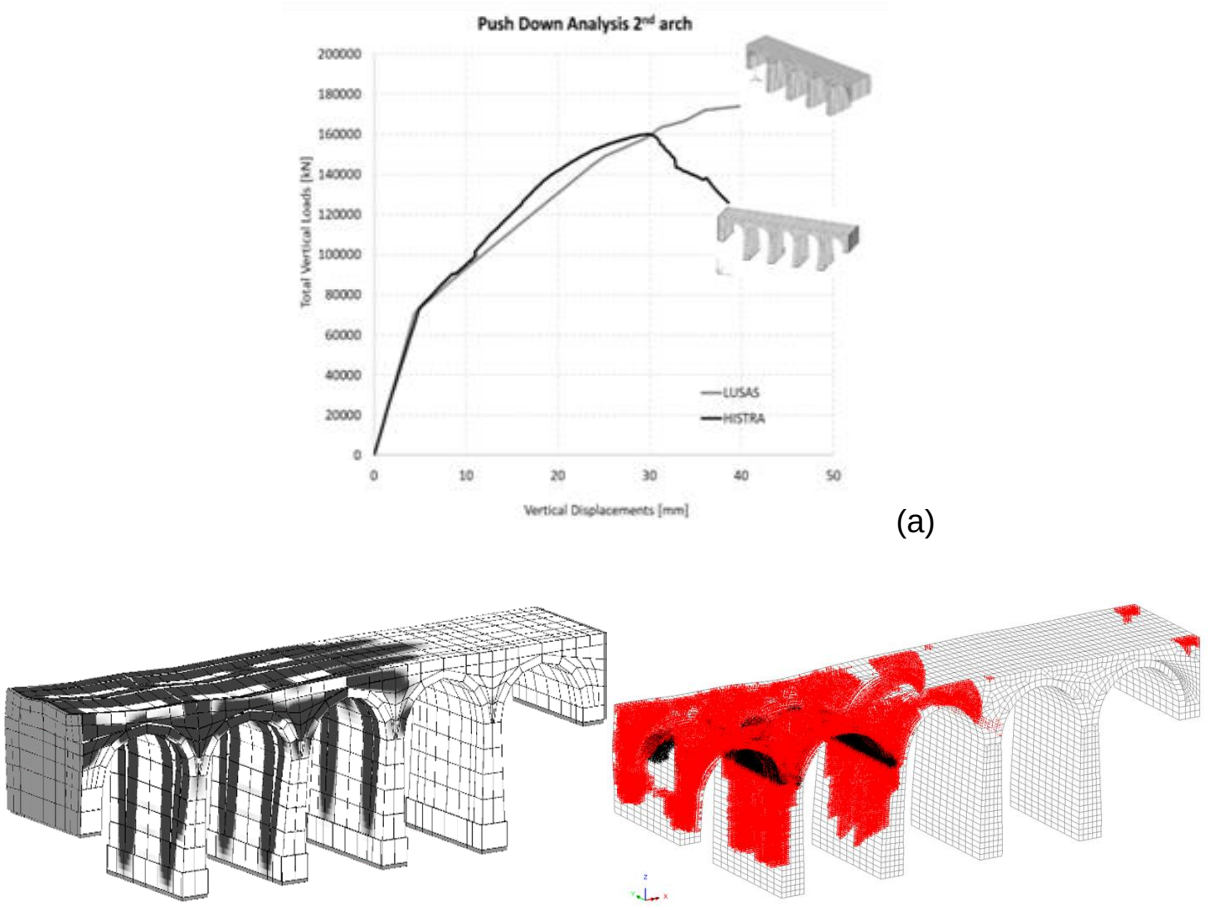

Figure 16. Comparison in terms of (a) capacity curves and damage pattern at collapse according to (b) proposed and (c) the FE approaches.